# Static Distortion of $^2E_g$ Cyclohexane Cation Radicals giving the $^2A_g$ State with $C_{2h}$ Symmetry and their Dynamic Processes in Low-temperature Solids: Matrix Effects

**Kazumi Toriyama, Keichi Nunome, and Machio Iwasaki**

*Government Industrial Research Institute, Nagoya, Hirate, Kita, Nagoya 462, Japan*

E.s.r. evidence has been obtained showing that the Jahn–Teller active radical cation of cyclo-$C_6H_{12}$ exhibits static distortion to the $^2A_g$ ground state with $C_{2h}$ symmetry in low-temperature solids regardless of the matrix used; non-isotropic perturbation by the matrix results in a nonequivalent dynamic process in the Jahn–Teller potential surface which has three minima.

The direct observation of Jahn–Teller distortion of symmetrical radical cations is of interest in radical ion chemistry. We have previously determined the distorted structures of $C_2H_6^+$, $CHMe_3^+$, $CMe_4^+$, cyclo-$C_3H_6^+$, cyclo-$C_4H_8^+$, and $C_6H_6^+$ by matrix e.s.r. spectroscopy at low temperature.[1] In such solid-phase studies, however, the perturbation by the matrix to the distortion must be carefully examined. In the present work we have studied the matrix effects on the distortion of radical cations of cyclohexane[2,3] using a variety of matrices [$CFCl_3$, $CFCl_2CF_2Cl$, $CF_3CCl_3$, cyclo-$C_6F_{12}$, cyclo-$C_6F_{10}(CF_3)_2$, *etc.*], in which the cations were radiolytically produced.[1–6]

Shown in Figures 1(a) and 1(b) are the spectrum of cyclo-$C_6H_{12}^+$ observed in $CFCl_3$ at 4.2 K immediately after irradiation at 4.2 K and the simulated spectrum. Although the observed spectra at 4.2 K vary considerably from matrix to matrix, all the spectra can be simulated by the three sets of two equivalent couplings. A typical example is shown for $CFCl_3$ in Figure 1(b).† The three sets of coupling constants observed in different matrices are plotted against the largest coupling constants in Figure 2.

Now, the $e_g$ highest occupied orbital of cyclo-$C_6H_{12}^+$ with $D_{3d}$ symmetry[8] splits into $a_g$ and $b_g$ orbitals by $C_{2h}$ distortion along the Jahn–Teller-active $e_g$ modes as shown in Figure 3(a). Because of the σ bonding nature of C(2)–C(3) [C(5)–C(6)] in the $a_g$ orbital, elongation and compression of the two parallel C–C bonds lead to the $a_g$ and $b_g$ SOMO, respectively. INDO MO calculations show that the equatorial protons participating in the SOMO exhibit a large hyperfine coupling, giving two large [102 G for C(1) and C(4) protons] and four small [18 G for C(2), C(3), C(5), and C(6) protons] couplings for $a_g$, whereas there are four large [71 G for C(2), C(3), C(5), and C(6) protons] couplings for $b_g$.‡ If the small difference in the two smaller sets (34 and 14 G) of observed couplings in $CFCl_3$ is ignored compared with the largest coupling of 85 G, the observed spectrum indicates that the $^2A_g$ state is the ground state. The large positive $g$ shift along the molecular axis ($g_\parallel$ = 2.0111) is due to excitation from the near-degenerate lower level of $b_g$ by $L_z$.

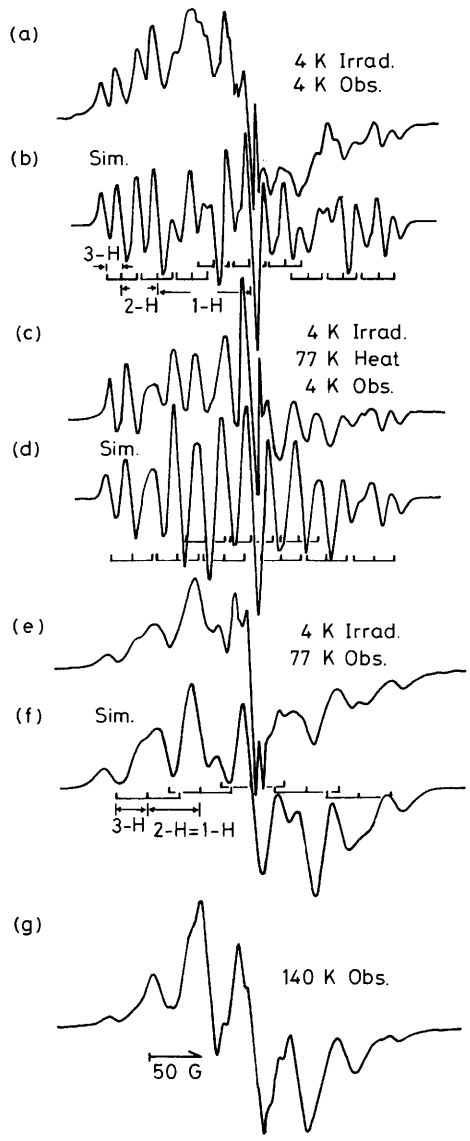


**Figure 1.** (a) E.s.r. spectrum of cyclo-$C_6H_{12}^+$ in $CFCl_3$ observed at 4.2 K immediately after irradiation at 4.2 K; (b) simulation for (a) using $A_\parallel$ = 88.7 G, $A_\perp$ = 83.2 G for 1-H, $A_\parallel$ = 37.6 G, $A_\perp$ = 32.2 G for 2-H, $A_\parallel$ = 17.6 G, $A_\perp$ = 12.2 G for 3-H, $g_\parallel$ = 2.0111, and $g_\perp$ = 2.0023; (c) spectrum observed at 4.2 K after annealing at 77 K; (d) simulation for (c) using $A_\parallel$ = 71.7 G, $A_\perp$ = 66.2 G for 1-H, $A_\parallel$ = 48.6 G, $A_\perp$ = 43.2 G for 2-H, $A_\parallel$ = 21.0 G, $A_\perp$ = 16.2 G for 3-H, $g_\parallel$ = 2.0111, and $g_\perp$ = 2.0023; (e) spectrum observed at 77 K; (f) simulation for (e) using $a_{iso}$ = 50 G for 1-H and 2-H, 29 G for 3-H with isotropic $g$ value; (g) spectrum observed at 140 K. The $A_\parallel$ axis is along the C–H bond and $g_\parallel$ along the molecular axis. 1 G = $10^{-4}$ T. The stick diagrams given under the simulated spectra illustrate the isotropic line positions.

† The parameters used for the spectral simulations are given in the caption to Figure 1. The dipolar tensors were estimated by two-centre integrals using Slater orbitals by the method employed by Barfield.[7] The INDO spin density distributions were assumed to produce the resultant dipolar tensors. Since the calculated magnitudes of the dipolar tensors were nearly the same for the three kinds of coupling protons, the same averaged tensor with axial symmetry was assumed, although the parallel principal directions are taken to be along each C–H bond.

‡ The INDO values for the $^2A_g$ and $^2B_g$ states were obtained for distortions along the Jahn–Teller-active $e_g$ C–C stretching mode by +0.02 and −0.02 Å, repectively, from the symmetrical structure with $r_{CC}$ = 1.48 Å, which lowers the total energy, rather than the normal value of 1.54 Å. Tetrahedral bond angles and $r_{CH}$ = 1.09 Å were assumed.

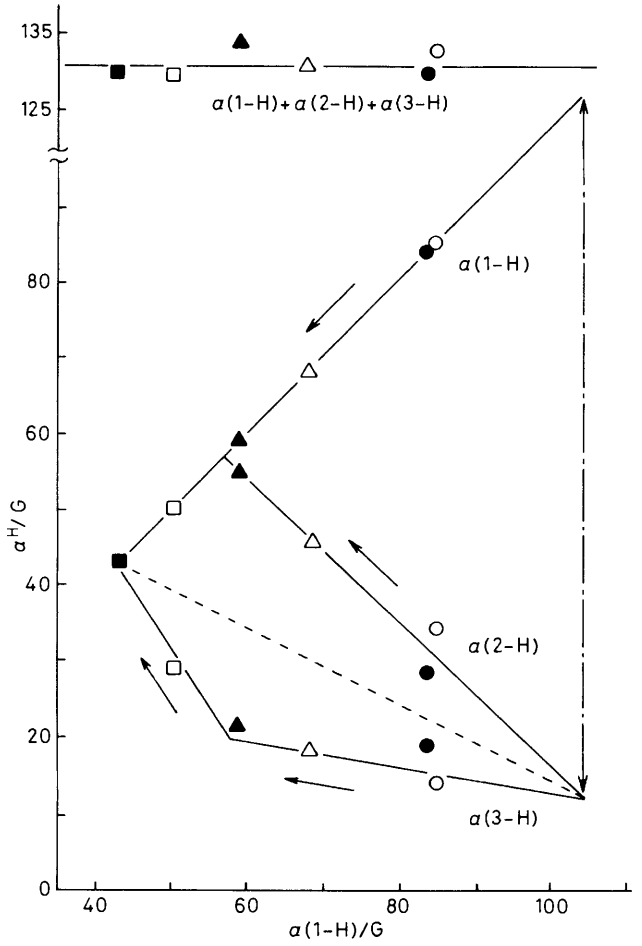


**Figure 2.** Variations of isotropic hyperfine coupling constants for 1-H(4-H), 2-H(6-H), and 3-H(5-H) plotted against the largest coupling constant. ○: observed at 4.2 K in $CFCl_3$ immediately after irradiation at 4.2 K; △: observed at 4.2 K in $CFCl_3$ after annealing at 77 K; □: observed at 77 K in $CFCl_3$; ■: observed at 140 K in $CFCl_3$; ●: observed at 4.2 K in $CF_3CCl_3$ immediately after irradiation at 4.2 K; ▲: observed at 4.2 K in $CFCl_2CF_2Cl$ immediately after irradiation at 4.2 K. Spectra observed in cyclo-$C_6F_{12}$ and in cyclo-$C_6F_{10}(CF_3)_2$ give similar coupling constants to those in $CFCl_2CF_2Cl$.

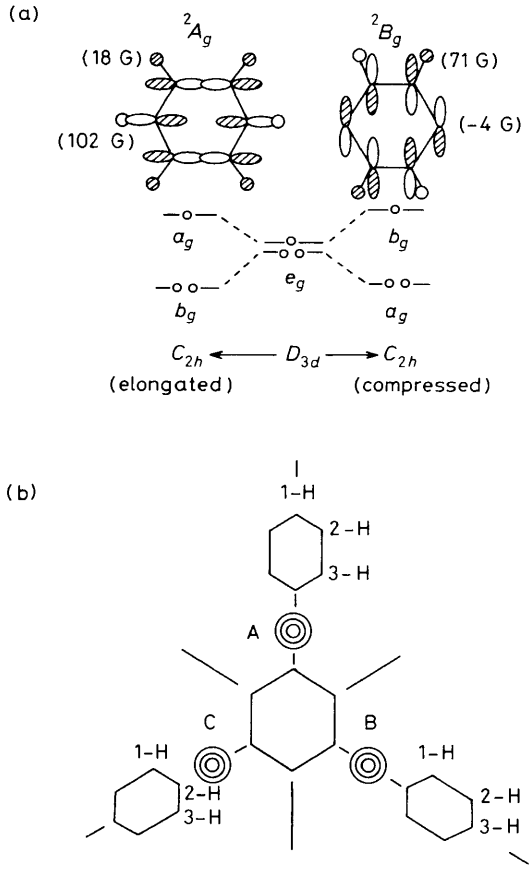


**Figure 3.** (a) The unpaired electron orbitals for the $^2A_g$ and $^2B_g$ states. The numbers in parentheses are the hyperfine coupling constants calculated by the INDO MO method; (b) schematic representation of the three minima on the Jahn–Teller potential surface.

After annealing the sample at 77 K, the spectra change irreversibly in most of the matrices used. A typical example is given in Figure 1(c) [simulation in Figure 1(d)]. After the annealing the difference between the two small couplings is enhanced as shown in Figure 2. Once the samples have been annealed at 77 K, the spectra exhibit reversible temperature changes in the range 4.2—140 K. The spectrum measured in $CFCl_3$ shows that the two sets of coupling constants become equivalent at 77 K [Figure 1(e)] and all the three sets become equivalent giving an equally spaced seven-line spectrum at 140 K [Figure 1(g)].

As shown in Figure 2, the three sets of coupling constants vary in such a way that the two smaller sets increase linearly as the largest coupling decreases, regardless of the matrix used and of the annealing at 77 K. Since the sum of the coupling constants is invariant for all the spectra, the apparent difference in the coupling constants must arise from the difference in the extent of the motional averaging of the coupling constants. Extrapolation of the straight lines for the two sets of small coupling constants in Figure 2 indicates that the point giving the same values for 2-H and 3-H corresponds to the rigid state, in which $a$(2-H) = $a$(3-H) = 13 G and $a$(1-H) = 103 G. These values are in good agreement with the INDO values (18 and 102 G) calculated for the $^2A_g$ state. The non-equivalence of 2-H and 3-H at 4.2 K suggests that partial averaging takes place to some extent by zeropoint vibrations.

The Jahn–Teller potential surface of the distorted cations possesses three equivalent minima corresponding to the three equivalent directions of the deformations [Figure 3(b)].[9] The onset of jumping between these equivalent minima must not lead to the non-equivalence of 2-H and 3-H and the small coupling must vary along the dotted line shown in Figure 2. In the solid phases, however, the trapping site may not be isotropic. So, it is likely that the rates of jumping from one of the three minima to the two neighbouring minima are different from each other, if the site symmetry is lower than $C_3$. This may explain why the averaging of $a$(1-H) and $a$(2-H) takes place more rapidly than the averaging of $a$(1-H) and $a$(3-H), as is observed.

These results obtained from a variety of matrices indicate that at least under conditions such that the cations are confined to the matrix cavity, the Jahn–Teller instability results in the $^2A_g$ ground state regardless of the matrix used. However, the Jahn–Teller potential surface depends upon the

matrix conditions and the perturbation by the matrix results in the non-equivalence of the three potential minima.

*Received, 13th September 1983; Com. 1224*

## References

1 M. Iwasaki, K. Toriyama, and K. Nunome, *J. Am. Chem. Soc.*, 1981, **103**, 3591; K. Toriyama, K. Nunome, and M. Iwasaki, *J. Chem. Phys.*, 1982, **77**, 5891; M. Iwasaki, K. Toriyama, and K. Nunome, *J. Chem. Soc., Chem. Commun.*, 1983, 202, 320; K. Ushida, T. Shida, M. Iwasaki, K. Toriyama, and K. Nunome, *J. Am. Chem. Soc.*, 1983, **105**, 5496.
2 T. Shida and Y. Takemura, *Radiat. Phys. Chem.*, 1983, **21**, 157.
3 M. Tabata and A. Lund, *Chem. Phys.*, 1983, **75**, 379.
4 T. Shida, Y. Egawa, H. Kubodera, and T. Kato, *J. Chem. Phys.*, 1980, **73**, 5963.
5 M. C. R. Symons, *Chem. Phys. Lett.*, 1980, **69**, 198.
6 K. Toriyama, K. Nunome, and M. Iwasaki, *J. Phys. Chem.*, 1981, **85**, 2149.
7 M. Barfield, *J. Chem. Phys.*, 1970, **53**, 3836; 1971, **55**, 4682.
8 W. L. Jorgensen and L. Salem, 'The Organic Chemist's Book of Orbitals,' Academic Press, New York, 1973, p. 278.
9 G. Herzberg, 'Molecular Spectra and Molecular Structure III. Electronic Spectra and Electronic Structure of Polyatomic Molecules,' Van Nostrand Reinhold, New York, 1966, p. 50.